



Tuning the sorption properties of amidoxime-functionalized algal/polyethyleneimine beads for La(III) and Dy(III) using EDTA: Impact of metal speciation on selective separation

Yue Zhang, Mohammed Hamza, Thierry Vincent, Jean-Claude Roux,
Catherine Faur, Guibal Eric

► To cite this version:

Yue Zhang, Mohammed Hamza, Thierry Vincent, Jean-Claude Roux, Catherine Faur, et al.. Tuning the sorption properties of amidoxime-functionalized algal/polyethyleneimine beads for La(III) and Dy(III) using EDTA: Impact of metal speciation on selective separation. *Chemical Engineering Journal*, 2022, 431 (Part 3), pp.133214. 10.1016/j.cej.2021.133214 . hal-03412398

HAL Id: hal-03412398

<https://imt-mines-ales.hal.science/hal-03412398>

Submitted on 8 Nov 2021

HAL is a multi-disciplinary open access archive for the deposit and dissemination of scientific research documents, whether they are published or not. The documents may come from teaching and research institutions in France or abroad, or from public or private research centers.

L'archive ouverte pluridisciplinaire **HAL**, est destinée au dépôt et à la diffusion de documents scientifiques de niveau recherche, publiés ou non, émanant des établissements d'enseignement et de recherche français ou étrangers, des laboratoires publics ou privés.

Tuning the sorption properties of amidoxime-functionalized algal/polyethyleneimine beads for La(III) and Dy(III) using EDTA: Impact of metal speciation on selective separation

Yue Zhang ^{a,c}, Mohammed F. Hamza ^d, Thierry Vincent ^a, Jean-Claude Roux ^b, Catherine Faur ^c, Eric Guibal ^{a,*}

^a PCH, IMT Mines Alès, Alès, France

^b C2MA, IMT Mines Alès, Univ. Montpellier, Alès, France

^c IEM, Institut Européen des Membranes, Univ. Montpellier, CNRS, ENSCM, Montpellier, France

^d Nuclear Materials Authority, POB530, El-Maadi, Cairo, Egypt

A B S T R A C T

Amidoximated algal/polyethyleneimine beads are successfully applied for the sorption of two rare earths elements (REEs, Ln(III)): La (light) and Dy (heavy). The sorption properties are characterized by FTIR and SEM-EDX analyses. The pH effect on metal sorption is investigated with a double objective: optimizing metal recovery and separation. In binary solutions, Dy(III) shows slightly higher affinity for the sorbent than La(III); without significant differences in the selectivity. The difficult separation of REEs can be modulated using EDTA. Playing with the pH and the concentration of the ligand, La(III) can be separated from Dy(III). Selectivity coefficient, $SC_{La/Dy}$, may reach up to 40–50. Speciation diagrams show that the preferential formation of Dy-EDTA complexes limits Dy(III) sorption while La(III) remains predominant and highly sorbed (reduced effect of Dy-competition). Optimum conditions for Ln(III) separation can be predicted by the calculation of speciation diagrams. The concept is verified for the separation of La(III) from Er(III) (heavy REE). In the presence of EDTA, sorption isotherms (mono-component solutions) present sigmoidal shapes due to the effect of metal complexation. Converting the total concentration to the concentration of sorbable species (non-complexed by EDTA) allows plotting favorable curves (Langmuir equation). The fits of experimental profiles with the modified Langmuir equation confirm the preference of the sorbent for non-complexed species. The kinetic profiles fitted by the Crank equation highlight the contribution of the resistance to intraparticle diffusion in the control of uptake kinetic; this effect is reinforced by the presence of EDTA. Metal desorption using $CaCl_2$ (50 mM, pH 2) or EDTA (0.5 mM, pH 6) is used for La(III) and Dy(III) desorption (yield: 80–95%), while sorption capacity progressively decreases over 3 cycles.

Keywords:

Increased affinity of La(III) and Dy(III) for amidoximated algal/PEI beads

Enhanced separation of light vs. heavy REEs in presence of EDTA, due to preferential complexation of heavy rare earth elements

Correlation between preferential sorption and metal speciation

Modified Langmuir equation for fitting sorption isotherms (taking into account only the concentration of adsorbable free metal species)

1. Introduction

1.1. Strategic issue of the separation of REEs

The growing demand of rare earth elements (REEs) is driven by the development of High Tech furniture (alloys, super magnets, electronic and optoelectronic devices, and so on) [1]. The production of these strategic metals is limited to a few countries; therefore, developing processes for recovering these metals from low-grade ores, secondary sources, by-products and wastes (including the so-called WEEEs, waste electric and electronic equipment) became a strategic issue in the last

decades [2–4]. This increasing pressure on resources, the environmental constraints, and the geostrategic issues may explain the incentive policies proclaimed at national or regional levels for developing virtuous production and management of base metals, radionuclides, precious and strategic metals.

For these reasons, many studies have been developed all over the world for recovering REEs with management of selective leaching from low-grade metal resources, development of new extractants [5–7] and sorbents such as nanomaterials [8,9], chelating resins [10–13], ion-exchange resins [14–16] and more generally flow sheets for effective valorization of these metals [17]. However, one of the most critical

* Corresponding author.

E-mail address: Eric.Guibal@mines-ales.fr (E. Guibal).

challenges remains the separation of these metals. Indeed, the members of the REE family (from La to Lu, completed with two other metals having similar behavior and frequently associated with REEs in geological resources: Sc and Y) have very similar physicochemical properties. Therefore, their selective separation usually requires extensive methods of purification for achieving the selective recovery of individual REEs and producing the purity standards required for High Tech applications [18–19]. Different strategies have been proposed based on selective methods of leaching [20,21], solvent extraction [22], or precipitation [23,24] for the recovery of metals from ores and solid wastes.

The close values of ionic radius of the REE make their size-based separation very challenging [1]. These methods require numerous theoretical plateaus for liquid/liquid separation or using sophisticated techniques like vapor phase extraction [25–27].

In the field of sorption processes (which are more appropriate for the treatment of low concentration solutions), ion-exchange, chelating or impregnated resins have been widely investigated [15,28]. The structuration of the sorbent, playing with the specific surface area, the tunable pore size and the grafting of specific functional groups, constitutes very useful strategies for improving selective separation of REEs [29,30]. Florek et al. [31] designed silica-based sorbents decorated with diglycolamide (DGA) ligands; they demonstrated that the bite angle (angle formed between the metal and the ligand moieties) and the environment of DGA ligands allows enhancing the selective recovery of some REEs. Roosen et al. reported the EDTA (ethylene diamine tetra acetic acid) and DTPA (diethylene triamine pentaacetic acid) functionalization of chitosan-based composites for the sorption [32] and separation of rare earths [33]. Zhao et al. [34] synthesized a β -cyclodextrin derivatives where EDTA acts as both a cross-linker and a selective binder for REEs. Suzuki et al. [35] played with the addition of alcohols together with the concentration of nitric acid for the separation of REEs using tertiary pyridine-type resin. Similar beneficial effects of alcohol presence on selective separation were reported for benzimidazole-type anion exchange resins [36].

Historically, the use of soluble ligands has been frequently reported for improving the separation of rare earths in solvent extraction processes [37–44], more rarely with ion-exchange resins [45,46]. Different soluble ligands such as lactic acid [41,42], citric and formic acids [47], EDTA and analogues [28,48–50] were also investigated for the separation of REEs onto resins. However, to the best of our knowledge, this is the first time the modulation of REE speciation using EDTA is in deep investigated for developing the selective separation of light from heavy REEs. This separation is driven by the introduction of EDTA as a modulator of metal speciation. Playing with both the pH and the specific chelation of Dy(III) and La(III), it is possible to change their speciation in the solution, which, in turn, controls the affinity of the sorbent for target metals. Similar interpretations of modulation of metal sorption through metal speciation have been documented for copper recovery in the presence of citrate [51].

1.2. Rationale for designing functionalized algal/PEI sorbent (APEI)

Amine-enriched algal/alginate beads were prepared using an original method, reported by Wang et al. [52]. The beads (APEI) are prepared by partial extraction of alginate from brown algae (eventually enriched with external alginate biopolymer) and further reaction with polyethylenimine (PEI); the mixture was then dropped into a CaCl_2 /glutaraldehyde (GA) solution for ionotropic gelation of alginate and crosslinking of amine groups of PEI, to form spherical porous sorbents. Recently, a series of new sorbents based on the functionalization of algal, alginate and PEI beads have been recently developed, including the grafting of sulfonic [53], quaternary ammonium [54], phosphorous-based groups [55,56] for improving the sorption properties of the raw beads. The amidoximation of the beads (AO-APEI) was also efficient for enhancing Sr(II) sorption (including in complex seawater) [57]. The

same type of material is investigated in the current work for the sorption of La(III) and Dy(III), lanthanum being part of light REEs (LREE) while Dy is a member of heavy REEs (HREEs); retaining the objective to separate La(III) from Dy(III). The [Supplementary Material](#) Information (SI, Fig. S1) shows La(III) and Dy(III) sorption isotherms using raw APEI beads. Under comparable conditions, the maximum sorption capacities are almost doubled after amidoximation (see below)

1.3. Research methodology

The characteristics of amidoximated APEI beads (AO-APEI) have been already well documented in previous work (including TGA, FTIR and XPS characterizations of sorbent functionalization, BET, elemental analysis [57]). For this reason, this work focuses on the characterizations of interactions between AO-APEI and lanthanide(III) ($\text{Ln}(\text{III})$) using FTIR spectroscopy and semi-quantitative EDX (energy dispersive X-ray) analysis. The sorption properties are analyzed through the evaluation of the effect of pH, presence of EDTA, uptake kinetics, sorption isotherms (mono- vs. bi-component solutions), as well as metal desorption and sorbent recycling. Most of this information is available in the [Supplementary Information](#) (SI), in order to focus on the main objective of this work: optimizing the selective separation of La(III) from Dy(III), through the mediation of metal speciation using EDTA. The selectivity is discussed with reference to the speciation of metal ions in presence and absence of EDTA, while the sorption properties (uptake and isotherms) are modeled using conventional equations (reported in Annex I, SI). Complementary investigation extends the selective strategy to the separation of La(III) from La(III)-Er(III) and La(III)-Cu(II) bi-component solutions.

2. Materials and methods

2.1. Materials

Algal biomass came from preprocessed *Laminaria digitata* biomass (Setalg, Pleubian, France). Sodium alginate (namely Manugel GMB) was provided by DuPont (Landerneau, France; now JRS Rettenmaier). Organic reagents included branched polyethylenimine (PEI, 50% (w/w)), formic acid, glutaraldehyde solution (GA, 50%), chloroacetonitrile, and poly(ethyleneglycol) diglycidyl ether were purchased from Sigma-Aldrich (Taufkirchen, Germany). LaCl_3 , DyCl_3 , ErCl_3 , CuCl_2 , Ethylenediaminetetraacetic disodium salt dihydrate (EDTA-Na₂), K_2CO_3 , Na_2CO_3 and $\text{CaCl}_2 \cdot 2\text{H}_2\text{O}$, HCl, NaOH, methanol and HCOOH came from Chem-lab NV (Zedelgem, Belgium). The rest of reagents include isopropylalcohol (Carlo Erba, France), dimethylformamide (DMF) (Pan-Reac AppliChem ITW, Chicago, USA) and hydroxylamine hydrochloride (Fluka, Buchs, Switzerland). All solutions were prepared with deionized water.

The stock solutions of $\text{Ln}(\text{III})$ ($\text{La}(\text{III})$ or $\text{Dy}(\text{III})$ – 50 mmol L⁻¹) were prepared by dissolving appropriate amounts of LaCl_3 or DyCl_3 with deionized water, respectively; the stock solution of EDTA (50 mmol L⁻¹) was prepared by dissolving appropriate amounts of EDTA-Na₂ with deionized water.

The working solutions of [$\text{Ln}(\text{III})$] were prepared by dilution of $\text{Ln}(\text{III})$ stock solutions: the mono-component $\text{Ln}(\text{III})$ solutions were obtained by diluting $\text{La}(\text{III})$ or $\text{Dy}(\text{III})$ stock solution to the required concentration, while the bi-components $\text{Ln}(\text{III})$ solutions were obtained by mixing appropriate volume of $\text{La}(\text{III})$ and $\text{Dy}(\text{III})$ stock solutions. The working solutions of [$\text{Ln}(\text{III})$ -EDTA] were prepared by mixing appropriate volume of EDTA, $\text{La}(\text{III})$ and $\text{Dy}(\text{III})$ stock solutions.

2.2. Synthesis of sorbents

The original alginate/PEI beads were prepared through protocol of Wang et al. [52]. Briefly, a certain amount of *L. digitata* biomass was added into Na_2CO_3 solution and maintained at 50 °C for 24 h for internal

alginate extraction. Later, a mixture of alginate and PEI solution was added to stabilize the biopolymer and to increase the density of amine groups. Finally, the mixture was dropwise dropped into a cross-linking solution containing CaCl_2 for the ionotropic gelation of alginate fraction and GA for cross-linking amine groups from PEI. The interpenetrating network (alginate/Ca and PEI/GA) makes the raw beads highly stable.

Then, the amidoximation of alginate/PEI beads includes three major steps [57]:

(i) the original beads were reinforced by reaction of poly(ethylenglycol) diglycidyl ether (3 mL) in isopropyl alcohol (87 mL), under reflux for 4 h. After being rinsed with isopropyl alcohol and water, the reinforced beads (R-APEI) were vacuum-dried under $-101\text{ }^\circ\text{C}$ for 24 h;

(ii) the nitrilation of R-APEI was achieved in a mixture of dimethylformamide (DMF, 150 mL) and anhydrous potassium carbonate (20 g), under gentle agitation and reflux (at $70\text{ }^\circ\text{C}$) for 30 min. After cooling, chloroacetonitrile (15 mL) was added to the suspension and maintained under reflux for another 4 h. After rinsing with hot water and methanol (several times) to remove unreacted reagents, nitrated beads (N-APEI) were vacuum-dried under $-101\text{ }^\circ\text{C}$ for 24 h;

(iii) a solution was prepared by dissolving hydroxylamine hydrochloride (20 g) into ethanol/water (v:v = 5:1, 75 mL in total), the pH of the solution was adjusted to 9, using concentrated NaOH solution (to precipitate NaCl). Later, the filtrated solution was used for the amidoximation of the nitrated beads (N-APEI) under reflux (at $70\text{ }^\circ\text{C}$) for 5 h. Finally, amidoximated sorbent (AO-APEI) was recovered by filtration, rinsed with water and vacuum-dried under $-101\text{ }^\circ\text{C}$ for 24 h.

2.3. Characterization of sorbents

Fourier-transform infrared spectroscopy (FTIR) was performed in the range $4000\text{--}400\text{ cm}^{-1}$ using a Bruker VERTEX70 spectrometer (Bruker, Germany) equipped with a FTIR-ATR (Attenuated Total Reflectance tool). The morphology and structure of sorbents were characterized using an environmental scanning electron microscope (ESEM) Quanta FEG 200 (FEI France, Thermo Fisher Scientific, Mérignac, France), coupled with an Oxford Inca 350 energy dispersive X-ray (EDX) micro-analyzer (Oxford Instruments France, Saclay, France). The pH point of zero charge (pHpzc) of the beads was carried out by the so-called pH drift method [58].

2.4. Sorption tests for La(III) and Dy(III) sorption with EDTA tuning

All sorption experiments for mono- or bi-components Ln(III) solutions were conducted at room temperature ($20 \pm 1\text{ }^\circ\text{C}$) by contacting 0.5 g L^{-1} sorbents with desired concentrations of Ln(III) and EDTA solutions for 48 h (agitation speed was set to 150 rpm). Before contacting with the sorbents, the pH of each Ln(III) solution was adjusted to the required value using HCl or NaOH solution and was not controlled during the sorption process; however, the equilibrium pH was systematically monitored. Samples were collected at regular time intervals and filtered before being quantified by inductively coupled plasma atomic emission spectrometry (ICP-AES, JY Activa M, Jobin-Yvon, Horiba, Longjumeau, France). The specific conditions of the experiments are reported in the caption of each figure.

2.4.1. pH effect

The pH effect was investigated in the pH_0 range of 1–6, by contacting the sorbent with the mono- or bi- components Ln(III) solutions. Initial Ln(III) concentration (C_0 , mmol L^{-1}) was fixed at 0.5 mmol L^{-1} of mono-component solutions (La(III) or Dy(III)) or 1.0 mmol L^{-1} of bi-components solutions (La(III) and Dy(III) at equimolar concentrations), without or with a fixed concentration of 0.5 mmol L^{-1} EDTA. The equilibrium pH values were recorded on a pH-meter Cyber Scan pH 6000 (Eutech instruments, Nijkerk, the Netherlands). The samples were subsequently filtered through filter papers ($\varnothing 25\text{ mm}$, 1–2 μm pore size,

Prat-Dumas, France); the residual metal concentrations were analyzed by ICP-AES.

The sorption capacity (q_{eq} , mmol g^{-1}) was calculated by the mass balance equation:

$$q_{eq} = \frac{(C_0 - C_{eq})V}{m} \quad (1)$$

where m is the sorbent mass (g) and V the volume of solution (L); C_0 and C_{eq} are the initial and equilibrium concentrations (mmol L^{-1}), respectively.

2.4.2. Sorption isotherms

The sorption isotherms were evaluated at $\text{pH}_0 = 6$ by contacting the sorbent with the mono- or bi- components Ln(III) solutions, without or with a fixed concentration of 0.5 mmol L^{-1} EDTA in the solutions. For the mono-component Ln(III) solutions, batch sorption tests were performed by varying initial concentrations (C_0) from 0.1 to 1 mmol L^{-1} La(III) or Dy(III) solutions. For the bi-components Ln(III) solutions, the tests were performed in three parts:

(i) equimolar La(III) and Dy(III): La(III) and Dy(III) in concentrations (C_0) each varying from 0.1 and 1 mmol L^{-1} ;

(ii) varying La(III) with fixed Dy(III): La(III) in concentrations (C_0) varying from 0.1 and 1 mmol L^{-1} , while Dy(III) in concentrations (C_0) was fixed at 0.5 mmol L^{-1} ; and

(iii) varying Dy(III) with fixed La(III): Dy(III) in concentrations (C_0) varying from 0.1 and 1 mmol L^{-1} , while La(III) in concentrations (C_0) was fixed at 0.5 mmol L^{-1} .

2.4.3. Sorption kinetics

For uptake kinetics, the experiment was carried out at $\text{pH}_0 = 6$ in batch; a given amount of sorbents (i.e., 0.5 g) was contacted with 1 L of 1.0 mmol L^{-1} of bi-components Ln(III) solutions (La(III) and Dy(III) at equimolar concentrations); when relevant, EDTA was added at different concentrations (i.e., 0, 0.25 and 0.5 mmol L^{-1}). Samples were collected, filtrated and analyzed for residual metal concentrations.

2.4.4. Metal desorption and sorbent recycling

The study of Ln(III) desorption and sorbent reuse follows two steps:

(a) the sorption process was carried out at $\text{pH}_0 = 6$ by contact of the sorbent (sorbent dose: 0.5 g L^{-1} sorbent) with 1.0 mmol L^{-1} of bi-component Ln(III) solutions (La(III) and Dy(III) at equimolar concentrations). The residual concentrations of each Ln(III) were detected after reaching sorption equilibrium for the calculation of individual sorption capacities.

(b) for the desorption process, the Ln(III)-loaded sorbents (after being rinsed with water) were contacted with two different eluents (i.e., 50 mmol L^{-1} CaCl_2 at $\text{pH}_0 6$, and 0.5 mmol L^{-1} EDTA solutions at $\text{pH}_0 2$) for 12 h. The sorbent dose (SD) was the same as used for uptake kinetics. The desorbed concentrations of each Ln(III) were analyzed for calculation of desorption efficiencies of both La(III) and Dy(III).

After washing and drying, the regenerated sorbents were reused in the next cycle and three successively cycles of sorption–desorption were performed with the selected eluents.

The desorption efficiency (D_e , %) was evaluated by the amounts of metal already sorbed and afterwards desorbed:

$$D_e(\%) = \frac{(C_{eq} - C_{desorbed})}{C_{eq}} * 100 \quad (2)$$

where C_0 , C_{eq} and $C_{desorbed}$ are the initial, equilibrium and desorbed concentrations of Ln(III) (mmol L^{-1}) at each cycle, respectively.

For bi-component solutions, the sorption preference of AO-APEI for La(III) over Dy(III) was assessed by the selectivity coefficient ($SC_{La/Dy}$):

$$SC_{La/Dy} = \frac{q_{eq,La}C_{eq,Dy}}{q_{eq,Dy}C_{eq,La}} \quad (3)$$

3. Results and discussion

3.1. Summary of sorbent characterization and modes of interactions with REEs

Annex II (SI) reports the detailed characterization of the sorbent, as a specific complement to previous characterization of AO-APEI [57]. The sorbent is characterized as spherical beads (Table S1 and Fig. S2), with irregular surface due to shrinking mechanism during sorbent drying. The SEM observation of cross-sections confirms the high macroporosity of the beads (confirmed by measurements of apparent density) (Table S1). The scaffold structure (visualized through the distribution of C and O elements) is also observed in the SEM-EDX analyses (Table S2). Specific surface area was determined close to $40 \text{ m}^2 \text{ g}^{-1}$ [57]. The thermogravimetric analysis of AO-APEI beads showed a total weight loss close to 81%, associated with the residue of alginate/algal biomass/ CaCl_2 material [57].

In the Annex II (SI), the EDX cartography shows that the sorbent binds both La(III) and Dy(III) at both pH 3 and 6. While dysprosium is apparently localized onto the scaffold, lanthanum appears more homogeneously distributed in the cross section. In the presence of EDTA, Dy (III) partially disappears in the cross-section at pH 3 (and completely at pH 6); contrary to La(III) that remains distributed in the whole sorbent (with a higher density at pH 6 than at pH 3). These trends are confirmed by the semi-quantitative EDX analysis of the sorbents after metal sorption at pH 3 and 6 (Table S3). It is noteworthy that in the presence of EDTA, sodium cation is leached from the beads, while the relative mass fractions of C and O elements increase (probably due to partial electrostatic binding of EDTA).

The FTIR analysis (more extensively discussed in Annex II) allows identifying some changes associated with metal binding but also when the sorbent is mixed with an EDTA solution (without metal ions) (Fig. S3). As identified with EDX analysis, a partial electrostatic binding of EDTA on the sorbent affects the FTIR spectrum (mainly at the level of amine groups through interactions with carboxylate groups of the ligand). This is an important observation for the interpretation of metal binding in the presence of EDTA. The FTIR spectra after Ln(III) sorption at pH 3 and pH 6 show that the environments of amine (at $1595\text{--}1575 \text{ cm}^{-1}$), carboxylic (at 1720 cm^{-1}) and amidoxime groups (at 948 cm^{-1}) are affected by metal binding with different intensities depending on the pH and the presence of EDTA. These changes may be associated with the binding of either free metal ions or metal-EDTA complexes.

The comparison of pH_{PZC} values (obtained by the pH-drift method) showed the efficient functionalization of raw APEI beads: pH_{PZC} is shifted from 4.14 to 7.73 (Fig. S4). This means that AO-APEI beads will be fully protonated at both pH 3 and 6. This may be of critical importance for metal sorption through repulsive interactions for free cations or electrostatic attraction of anionic species.

3.2. Ln(III) sorption properties

3.2.1. Effect of pH on La(III) and Dy(III) sorption

The pH may affect the sorption performance and mechanism through different criteria dealing with metal speciation (see Annex III for detailed discussion of metal speciation in SI) and surface charge of the sorbent. Therefore, this is a parameter of critical importance for the investigation of metal sorption properties. Fig. 1 compares the sorption capacities for La(III) and Dy(III) (equimolar, 0.5 mmol L^{-1}) using AO-APEI in single-metal and binary solutions in absence (a) and presence (b) of EDTA (equimolar, 0.5 mM), as a function of equilibrium pH (i.e., pH_{eq}).

Sorption capacities increase with the pH, as expected from the acid-base properties and surface charge of the sorbents (see Section 3.1.). In absence of EDTA, the sorption of La(III) is negligible below pH 2 and linearly increases with the pH up to $\text{pH}_{\text{eq}} 6$; above pH 6, the steep

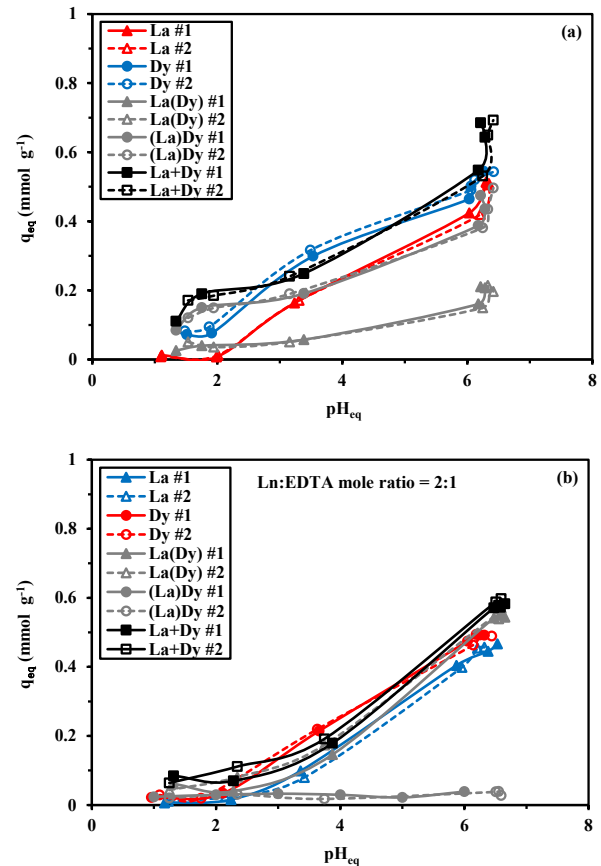


Fig. 1. Effect of pH on La(III) and Dy(III) sorption using AO-APEI beads from mono- and bi-component solutions in the absence (a) and in the presence (b) of EDTA ($\text{Co}_{\text{(metal)}}: 0.5 \text{ mmol L}^{-1}$; EDTA concentration: 0.25 mmol L^{-1} for mono-metal solutions and 0.5 mmol L^{-1} for binary solutions (when relevant); time: 48 h; SD: 0.5 g L^{-1} ; duplicate series: #1 and #2; La + Dy, corresponds to cumulative sorption capacities for binary solutions).

increase in sorption capacity is due to the formation of colloids and precipitates (this phenomenon is not observed in the presence of EDTA). Under selected experimental conditions, the sorption capacity rises to $0.42 \text{ mmol La g}^{-1}$ and $0.49 \text{ mmol Dy g}^{-1}$ at $\text{pH}_{\text{eq}} 6$, respectively in single-metal solutions. It is noteworthy that for Dy(III), the sorption capacities are not negligible (around $0.09 \text{ mmol Dy g}^{-1}$) in the range $\text{pH}_{\text{eq}} 1.5\text{--}2$; contrary to La(III). The profiles are drastically changed when the sorption is performed in binary equimolar solutions. The sorption of La(III) is strongly depreciated by the presence of Dy(III): the sorption capacity decreases to $0.15 \text{ mmol La g}^{-1}$ (reduced by 64%). On the opposite hand, the sorption capacity for Dy decreases by less than 23%. Surprisingly, at $\text{pH}_{\text{eq}} 1.5\text{--}2$ the sorption of Dy(III) is higher for binary than for mono-component solutions. The cumulative sorption capacity (q_{tot}) rises up to $0.53 \text{ mmol Ln g}^{-1}$ (close to the sorption capacity of Dy(III) in binary solutions), with remarkable inversion $q_{\text{tot}} > q_{\text{Dy(binary)}} > q_{\text{Dy(mono)}} > q_{\text{La(mono)}} > q_{\text{La(binary)}}$ at $\text{pH}_{\text{eq}} < 2$, and $q_{\text{Dy(mono)}} > q_{\text{tot}} > q_{\text{Dy(binary)}} > q_{\text{La(binary)}} > q_{\text{La(mono)}}$ at $\text{pH}_{\text{eq}} \sim 3.5$.

The presence of EDTA hardly influences the sorption of La(III) and Dy(III) in mono-component solutions: the profiles are almost superposed: negligible sorption at pH_{eq} below 2, and sorption capacity close to $0.46\text{--}0.49 \text{ mmol Ln g}^{-1}$ at $\text{pH}_{\text{eq}} 6.3$. In binary solutions, these trends are completely changed: the sorption of Dy(III) is drastically inhibited; the sorption capacity remains below $0.03 \text{ mmol Dy g}^{-1}$. On the other hand, the sorption of La(III) is almost unchanged and the cumulative sorption capacity almost overlaps with the La(III)-curve. These trends are consistent with the semi-quantitative EDX analyses of the sorbents (Table S3).

For both mono-component and binary solutions without EDTA, the speciation of the Ln(III) is not affected by the pH of the solution (free Ln^{3+} species, Fig. S5). Therefore the control of sorption performance is mainly driven by the deprotonation of reactive groups to decrease the ionic repulsion of cations by positively-charged surface (making possible the complexation of Ln^{3+} by amine, carboxylate and amidoxime groups). With the introduction of EDTA in the solution, the speciation of Ln(III) changes with formation of anionic LnEDTA^- species. It is noteworthy that the decrease in sorption properties in acidic solutions (at pH below 2) in the presence of EDTA may be explained by the supplementary competition effect of positively charged EDTA species (i.e., H_5EDTA^+ and $\text{H}_6\text{EDTA}^{2+}$). It is also noteworthy that the formation of anionic Ln(III) species is shifted toward lower pH values for Dy(III) compared with La(III). In binary solutions, at the highest pH values (the most favorable for metal binding), La^{3+} and DyEDTA^- species largely predominate in the solution. While La(III) is efficiently bound, sorption of Dy(III) does not exceed 0.03 mmol Dy g^{-1} . Free cationic Ln(III) species are more favorable to bind on AO-APEI beads than complexed anionic forms.

The presence of EDTA completely changes the preference of the sorbent for selected metals. In order to visualize this separation effect, the selectivity coefficients, $\text{SC}_{\text{La/Dy}}$, were calculated according:

$$\text{SC}_{\text{La/Dy}} = \frac{D_{\text{La}}}{D_{\text{Dy}}} = \frac{q_{\text{eq},\text{La}} \times C_{\text{eq},\text{Dy}}}{q_{\text{eq},\text{Dy}} \times C_{\text{eq},\text{La}}} \quad (16)$$

where D (L g^{-1}) is the distribution ratio, calculated from $D = q_{\text{eq}}/C_{\text{eq}}$.

Fig. 2 compares the $\text{SC}_{\text{La/Dy}}$ values as a function of pH_{eq} for solutions prepared without and with EDTA. In absence of EDTA, the sorbent has a weak preference for Dy(III), which is hardly influenced by the pH: the SC varies between 0.2 and 0.4. In presence of EDTA, the selectivity is reversed and considerably increased. In acidic solutions (i.e., pH_{eq} less than 4), $\text{SC}_{\text{La/Dy}}$ values range between 2 and 5–11. However, with the increase of the pH_{eq} (~6.5) the SC value increases up to 26–51. These effects are correlated to changes in the speciation of metal ions, and more specifically to the differences in the chelation of La(III) and Dy(III) by EDTA. The selectivity is improved for La(III), which is weakly chelated by EDTA compared with Dy(III) (see the discussion of metal speciation in Annex III). For further studies, the sorption was investigated at two pH values, representative of different conditions of surface charge for the sorbents and to different domains of predominance of metal species.

Fig. S15 reports the pH variation during metal sorption for mono-component solutions. Actually, the type of metal and the presence/absence of EDTA do not change the profiles of pH variation. Below pH_0

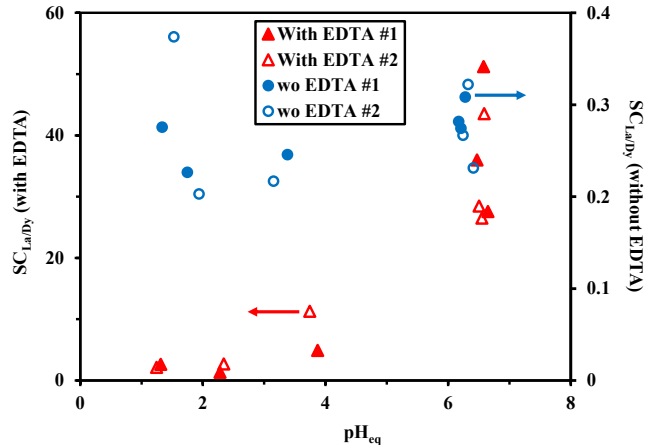


Fig. 2. Effect of the pH and the presence of EDTA on the selectivity of La/Dy sorption using AO-APEI beads (C_0 : 0.5 mmol L^{-1} ; EDTA concentration: 0.5 mmol L^{-1} (when relevant); time: 48 h; SD: 0.5 g L^{-1} ; duplicate series: #1 and #2).

= 3.4, the pH hardly varies (less than 0.4 pH unit); this may be explained by the weak sorption efficiency and the strong protonation of the sorbent (pH_{PZC} : 7.73), which limits the course of pH change in acidic solution. Between pH_0 3.5 and 4, a sharp increase in the pH is observed, corresponding also to the highest pH variation in the titration of the sorbent (pH-drift analysis in Fig. S5). The pH increases by about 2 pH units: the amplitude of pH change is consistent with the values reported in absence of metal ions.

3.2.2. Uptake kinetics

The uptake kinetics for La(III) and Dy(III) using AO-APEI at pH_0 6 is extensively discussed in Annex IV (SI) for both mono-component and binary solutions, in the absence and presence of EDTA. As a summary, it is possible to observe that:

(a) about 90% of total sorption occurs within the first four hours of contact.

(b) Dy(III) sorption (in mono-component solutions) is little better and faster than La(III) uptake using AO-APEI at pH_0 6.

(c) in binary solutions, in absence of EDTA, the differences in the profiles of Dy(III) (more efficient and much faster) and La(III) (compared with mono-component solutions) are more marked; associated with the preference of the sorbent for Dy(III) against La(III).

(d) in binary solutions with EDTA, the preference and kinetics are reversed: the sorption of La(III) is enhanced and the initial slopes are considerably increased (with increasing the concentration of EDTA); while the uptake of Dy(III) is progressively depreciated and almost completely inhibited at the highest EDTA concentration.

(e) the kinetic profiles are finely fitted by the pseudo-second order rate equation (PSORE) and to a lesser extent by the Crank equation (resistance to intraparticle diffusion, RIDE), which effect cannot be neglected (Figs. S16-S19 and Tables 1-2).

(f) the presence of EDTA decreases the effective diffusivity (probably due to the increased size of diffusing metal-ligand complex), making La (III) sorption faster than Dy(III) removal (dysprosium being complexed contrary to lanthanum).

(g) the faster sorption of lanthanum may be associated with the diffusivity coefficient of La(III) in water and by its greater affinity for the sorbent (rather than by the effect of the ionic radius of hydrated metal ions).

3.2.3. Sorption isotherms

Fig. 3 reports the sorption isotherms for La(III) and Dy(III) at pH_0 6 for mono-component (Fig. 3a,b, in presence and absence of 0.5 mM EDTA) and binary solutions (both equimolar concentrations (Fig. 3c,d) and with variable concentration of the competitor metal ion (Fig. 3e,f)). In absence of EDTA, the presence of Dy(III) drastically reduces the sorption capacity of La(III) (Fig. 3c,e): the maximum sorption capacity is

Table 1

Parameters for the modeling of uptake kinetics from mono-component solutions at pH_0 6.

Model	Metal ion	La(III)		Dy(III)	
		Parameter	Series	#1	#2
Experimental	$q_{\text{eq},\text{exp.}}$			0.582	0.597
PFORE	$q_{\text{eq},1}$			0.539	0.543
	$k_1 \times 10^2$			2.56	2.18
	R^2			0.953	0.961
	AIC			-86	-87
PSORE	$q_{\text{eq},2}$			0.582	0.589
	$k_2 \times 10^2$			6.84	5.62
	R^2			0.984	0.987
	AIC			-104	-105
RIDE	$D_e \times 10^9$			6.08	4.86
	R^2			0.989	0.990
	AIC			-102	-100

Units: q_{eq} : mmol L^{-1} ; k_1 : min^{-1} ; k_2 : g mmol $^{-1} \text{ min}^{-1}$; D_e : $\text{m}^2 \text{ min}^{-1}$.

Table 2Parameters for the modeling of uptake kinetics from binary (0.5 mmol L⁻¹ equimolar) solutions at pH₀ 6 in absence and presence of EDTA (0.25 mM).

Model	EDTA		Without		With 0.25 mM		With 0.5 mM	
	Parameter	REE	La(III)	Dy(III)	La(III)	Dy(III)	La(III)	Dy(III)
PFORE	q _{eq,exp.}		0.235	0.441	0.369	0.264	0.580	0.036
	q _{eq,1.}		0.216	0.405	0.344	0.246	0.544	0.033
	k ₁ × 10 ²		1.30	0.90	0.96	0.68	1.39	0.60
	R ²		0.977	0.960	0.977	0.986	0.983	0.914
PSORE	AIC		-139	-107	-123	-140	-118	-178
	q _{eq,2.}		0.240	0.460	0.390	0.287	0.602	0.039
	k ₂ × 10 ²		7.90	2.66	3.37	2.90	3.42	17.9
	R ²		0.995	0.982	0.994	0.995	0.998	0.926
RIDE	AIC		-167	-121	-147	-159	-151	-181
	D _e × 10 ⁹		4.17	2.36	2.90	2.27	3.32	2.29
	R ²		0.990	0.988	0.995	0.997	0.998	0.927
	AIC		-148	-125	-147	-165	-142	-183

Units: q_{eq}: mmol L⁻¹, k₁: min⁻¹; k₂: g mmol⁻¹ min⁻¹; D_e: m² min⁻¹.

halved and the initial slopes (which are correlated with the sorbate affinities for the sorbent) are reduced. This is consistent with previous conclusions that showed the preference of AO-APEI for Dy(III) against La (III). On the opposite hand, the sorption of Dy(III) is weakly affected by the presence of La(III) (even in excess) (Fig. 3d,f).

Furthermore, in the binary sorption of equimolar La and Dy, AO-APEI prefers binding Dy rather than La (0.26 mmol La g⁻¹ and 0.48 mmol Dy g⁻¹). Due to the so called lanthanide contraction [59], the ionic radius light REE La(III) ion is 1.06 Å, which is larger than that of heavy REE Dy(III) ion (0.91 Å). This contraction is a consequence of the incomplete charge shielding effect by the inner electrons on the 4f electronic shell on the heavier lanthanides, leading to a larger nuclear attractive force for the outer electrons. The higher charge density of Dy (III) ions show stronger electrostatic interactions with EDTA⁴⁻ ligands in the competition coordination with La(III) ions. As a result, the sorption property of La was strongly decreased in the presence of Dy.

The presence of EDTA strongly modifies these profiles (Fig. 3). For mono-component solutions, the isotherm begins with an unfavorable shape: the complexation of Ln(III) with EDTA makes the metals poorly adsorbable. When the concentration of the metal exceeds 0.5 mM (i.e., the same concentration as the ligand), free Ln³⁺ species begin to appear in the solution (Figs. S10 and S11) and the sorption progressively increases up to the sorption capacities reached with mono-component solutions (EDTA-free). In the case of La(III) sorption, the isotherm for binary solutions reveals more favorable than that of La(III) in mono-component solutions. Actually, the presence of Dy(III), which is readily complexed with EDTA (Fig. S8), displaces the speciation of La (III)-EDTA complex to the formation of free La(III) (consumption of EDTA and dissociation of La-EDTA complex). Therefore, the speciation of La(III) is more favorable for efficient sorption onto AO-APEI and the curve turns back to favorable sorption isotherm. On the opposite hand, Dy(III) sorption isotherms are very close in absence and presence of La (III) competitor ion. The preference of EDTA for complexing Dy(III) makes dysprosium speciation unaffected by the introduction of La(III) and the sorption isotherm remains non-favorable, indifferently of the composition of the solution (La with equimolar or variable concentrations). Adding soluble EDTA into the La-Dy binary system, La(III) sorption is partially restored (back to 0.53 mmol La g⁻¹). According to the known formation constants between EDTA with metals, EDTA selectively chelates with heavy REEs (HREEs, i.e., Dy) over light REEs (LREEs, i.e., La). Previous studies on the stability constants of LnEDTA⁻ chelates (i.e., log K_{LnEDTA}), measured by potentiometric titrations, showed very distinct values such as 18.28 for DyEDTA⁻ chelates and 15.46 for LaEDTA⁻ chelates [60].

In Fig. 3e,f (with fixed concentration of competitor Ln(III)), the presence of EDTA that complexes Dy(III) (preferentially to La(III)) allows restoring the favorable profile of La(III) sorption isotherm. In the case of Dy(III), the sorption is inhibited at low concentration because of the

complexation of the metal. When exceeding the Dy/EDTA equimolarity; the sorption increases but the maximum sorption capacity remains below than the values reported for mono-component solutions. This is due to the competitive sorption of La(III) which remained free in solution.

Fig. S20 compares the modeling of sorption isotherms with the Langmuir, the Freundlich and the Sips equations for mono-component solutions. Table 3 summarizes the parameters of the models (together with the statistical criteria). The asymptotic trends of the isotherm confirm that the Freundlich equation (power-type function) is not appropriate for fitting experimental profiles. The Langmuir and the Sips equations fit much better the profiles. The Langmuir equation supposes that the sorption occurs as a monolayer at the surface of the sorbent without interactions of sorbed molecules and with homogeneous distribution of sorption energies. The Sips equation combines the Langmuir and the Freundlich equations; this empirical equation usually allows fitting better mathematically the highly-curved part of the isotherm but fails to represent effective physicochemical mechanisms. The two models evaluate the sorption capacities at saturation of the sorbent relatively well (compared with experimental values; the differences are less than 8%): the maximum sorption capacities are close to 0.6 mmol Ln g⁻¹. The affinity coefficients (b_L and b_S) are systematically higher for La (III) than for Dy(III).

Table S5 compares La(III) and Dy(III) sorption properties of AO-APEI with a series of sorbents (biosorbents, resins, MOF, composites and extractant impregnated materials). The diversity of operating conditions makes difficult the comparison. In some cases, the levels of concentration and pH values question on the occurrence of precipitation phenomena (and overestimation of sorption capacities). Some sorbents have outstanding sorption capacities and fast kinetics, such as grapefruit peel [61] and tangerine peel [62] (though the sorption are apparently incomplete), marine algal biomass [63] for La(III) (q_{m,L}: 1.1–1.23 mmol La g⁻¹), functionalized silica nanoparticles [64] or activated charcoal [65] for Dy(III) (q_{m,L}: 1.62–1.83 mmol Dy g⁻¹). AO-APEI shows relatively slow sorption kinetics and the maximum sorption capacities are intermediary (around 0.6 mmol Ln g⁻¹); however, the affinity coefficient shows very high values (1171–1901 L mmol⁻¹), among the highest values reported in literature for these metal ions.

Table 4 compares the selectivity coefficients of alternative sorbents involving LREEs and HREEs. In most cases, the data reported preference for HREEs but with SC_{HREE/La} values ranging between 2 and 4, which are comparable to those reported in this study, in the absence of EDTA (SC_{La/Dy}: 0.18–0.34). However, in the presence of EDTA (0.5 mM for 0.5 mM La(III) and Dy(III)), the competitive sorption onto AO-APEI gives values for SC_{La/Dy} that increase up to 43.51.

In the presence of EDTA, the mono-component sorption isotherms are characterized by a non-favorable shape (sigmoidal profile) (Fig. 4). This can be directly associated with the large predominance of non-

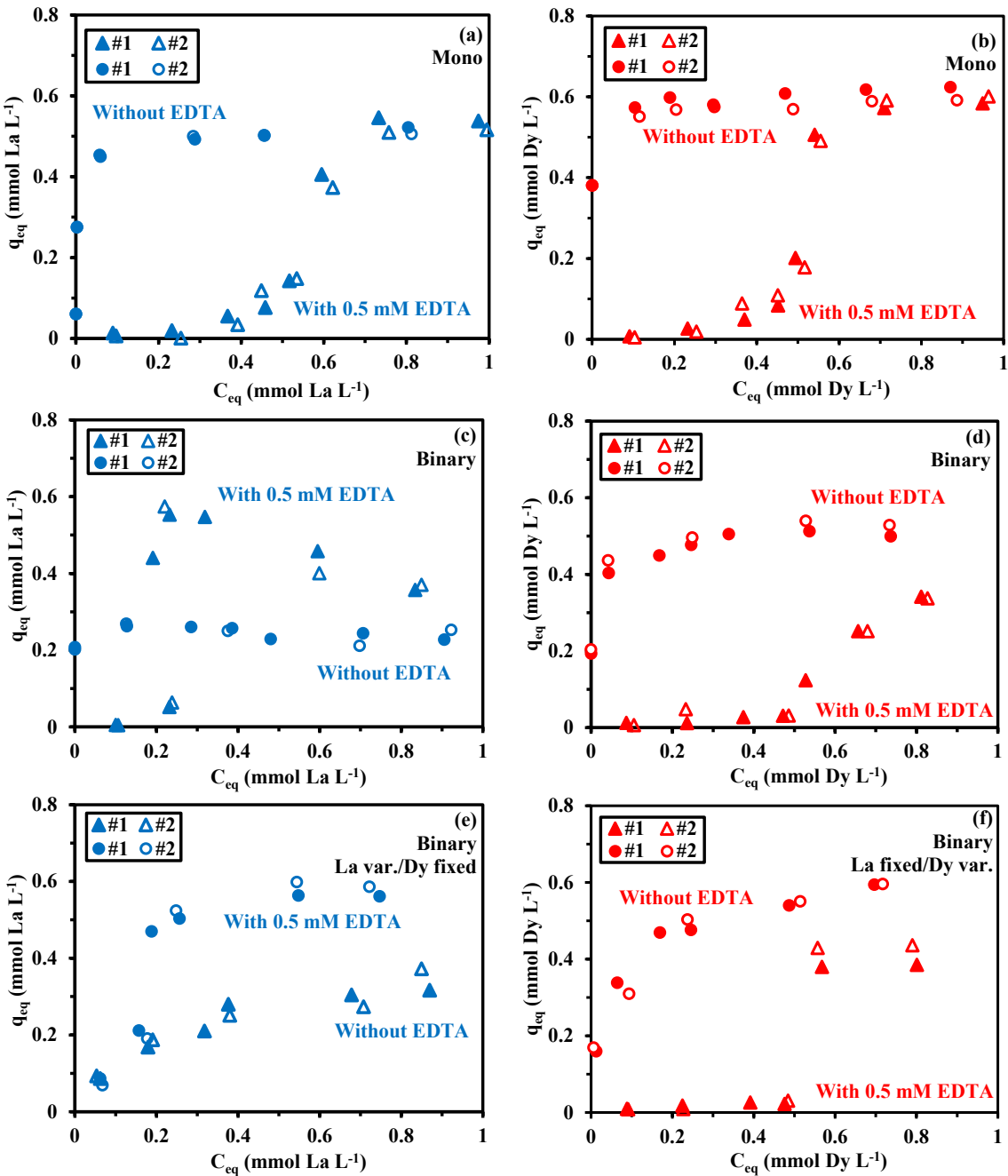


Fig. 3. La(III) (a, c, and e) and Dy(III) (b, d, and f) sorption isotherms at pH₀ 6 in presence and absence of EDTA (0.5 mM) for mono-component solutions (a and b), binary equimolar solutions (c and d), and binary solutions with variable La/Dy molar ratio (fixed D(III) concentration and variable La(III) concentration, and reciprocal; e and f). (SD: 0.5 g L⁻¹; contact time: 48 h; T: 20 ± 1 °C; duplicate series: #1 and #2).

adsorbable species (meaning EDTA-complexed forms) at low metal concentration: above $C_{eq} \sim 0.5$ mmol Ln L⁻¹. The quantitative complexation of Ln(III) with EDTA displaces the equilibrium to the formation of the complexes and the residual concentrations of sorbable species (meaning, La³⁺ and Dy³⁺ analogues) are negligible and the isotherm begins with a flat section. The sorption capacity begins to increase only when metal concentration exceeds 0.5 mmol Ln L⁻¹ (involving the formation of non-EDTA complexed species). The dotted lines in Fig. 4 represent the Langmuir modeling of experimental profiles converting the total concentration (C_{eq}) of Ln(III) into the effective concentration of sorbable species (C_{eq}^* , non EDTA-complexed species) and plotting q_{eq} vs. C_{eq}^* . The experimental points are shifted to the left and the non-favorable isotherm is turned into a very favorable isotherm

profile. Similar concept was applied to molybdate and vanadate sorption using chitosan-based sorbents [66,67].

Fig. S21 and S22 show the 3-D visualization of the sorption isotherms for mono-component and binary solutions (without EDTA) using q_{eq} as a function of two independent variables, $C_{eq,La}$ and $C_{eq,Dy}$. The optimized surface corresponds to the modeling of experimental data with the Competitive Langmuir and Competitive Sips equations, respectively. The parameters are summarized in Table S4. These visualizations clearly illustrate the differences in the cross-effects (competition) of La(III) and Dy(III) on their sorption capacities. The sigmoidal-type of the isotherms in the presence of EDTA does not allow applying these models for fitting experimental profiles.

Table 3

Parameters for the modeling of sorption isotherms in mono-component solutions at pH₀ 6.

Model	Metal ion Parameter	La(III)	Dy(III)
		q _{m,exp.}	0.565
Langmuir	q _{m,L}	0.547	0.576
	b _L	1901	1171
	R ²	0.989	0.946
	AIC	-54	-62
	k _F	7.36	10.0
Freundlich	n _F	0.641	0.664
	R ²	0.934	0.914
	AIC	-39	-68
	b _S	204.6	16.7
Sips	q _{m,S}	0.558	0.643
	b _S	1.37	2.56
	n _S	0.992	0.995
	AIC	-51	-97

Units: q_m: mmol g⁻¹; k_F: (mmol g⁻¹)·(L mmol⁻¹)ⁿ; b_L and b_S: L mmol⁻¹; n_F and n_S: dimensionless.

Table 4

Comparison of selectivity coefficients and sorption capacities with alternative systems.

Comparison	Sorbent	pH	Separation factor (SC _{Me1/Me2})	Ref.
REEs separation	Fe ₃ O ₄ @DTAF nanoparticles	3	2.5 for SF _{Dy/La}	[71]
	SiO ₂ @EDTA composites	6.5	2.6 for SF _{Dy/La}	[72]
	Fe ₃ O ₄ @SiO ₂ @TMS-EDTA nanoparticles	6	≈4 for SF _{Dy/La}	[73]
	Fe ₃ O ₄ @DTPA nanoparticles	6	2 for SF _{Nd/La}	[30]
	AO-Alginate/PEI beads	6	40.93 for SF _{La/Dy}	This study
REEs sorption	q _{m,exp.} (mmol g ⁻¹)			
	Fe ₃ O ₄ @DEHPA	5.5	0.40 for La(III)	[74]
	Fe ₃ O ₄ @humic acid	6.5	0.07 for Eu(III)	[75]
	Graphene-nanocomposite	4	0.36 for La(III)	[76]
	Straw-derived biochar	5	0.65 for La(III)	[77]
	Active carbons (spent coffee ground)	4	0.21 for Dy(III)	[78]
	Extractant-immobilized capsules	6	0.42 for Dy(III)	[79]
AO-Alginate/PEI beads	0.57 for La (III), 0.60 for Dy (III)			
	This study			

3.2.4. Effect of EDTA concentration on sorption capacity and selectivity

The comparative study of pH effect on the sorption and separation of La(III) and Dy(III) in the absence and presence of EDTA has highlighted the beneficial effect of Ln(III) differential complexation ability for selectively recovering La(III) (especially at pH₀ 6). The EDTA concentration remains an important parameter to optimize in terms of sorption capacity and selectivity. Fig. 5 shows the cross-effects of EDTA concentration and pH (3 and 6) on the sorption of Ln(III) and their separation. The curves have roughly the same shape, independently of the pH. At low EDTA concentration (around 0.1 mM), La(III) is weakly sorbed (0.04 mmol La g⁻¹) at least at pH 3 (around 0.28 mmol La g⁻¹ at pH 6) contrary to Dy(III) (0.26 and 0.38 mmol Dy g⁻¹ at pH 3 and 6, respectively). With increasing the concentration of the ligand, the sorption of dysprosium steeply decreases and becomes negligible while reaching EDTA: 0.5 mM. On the opposite hand, increasing EDTA concentration allows increasing the sorption of La(III) at least up to 0.5 mM, where a maximum is reached (with sorption capacities as high as 0.14 and 0.54 mmol La g⁻¹ at pH 3 and 6, respectively). The presence of increasing concentrations of EDTA improves the chelation of Dy; the formation of chelated species, which are less sorbable, makes more

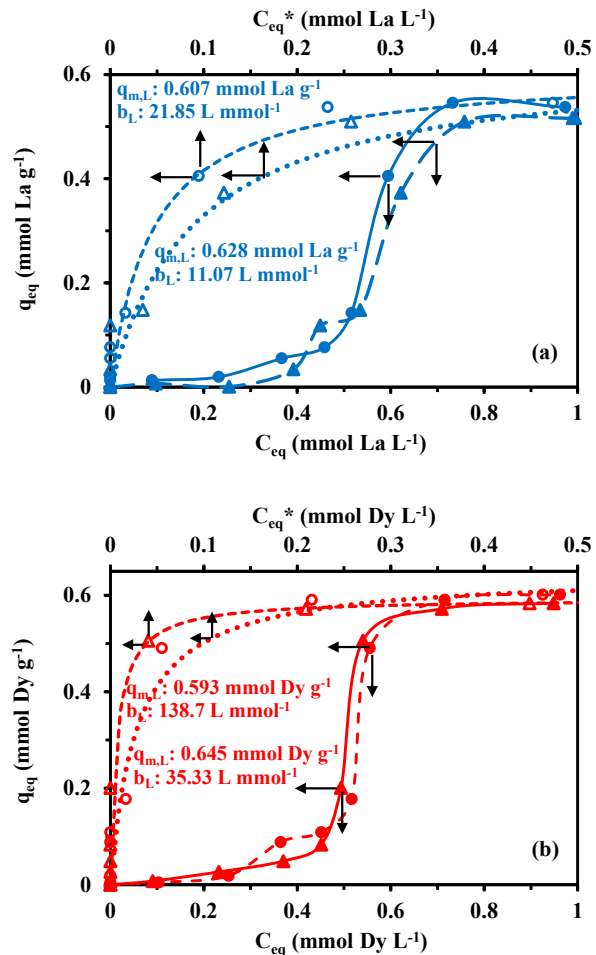


Fig. 4. Modeling of sorption isotherms (mono-component solutions at pH₀ 6; in the presence of 0.5 mM EDTA) with the modified-Langmuir equation (correcting the total metal concentration (C_{eq}) with the effective concentration of suggested adsorbable species (C_{eq}*): (closed symbols for q_{eq} = f(C_{eq}) (total La (III) concentration), open symbols for q_{eq} = f(C_{eq}*)) (C_{eq}*: [Ln³⁺] + [LnCl₂⁺] + [LnOH²⁺]), and dotted line: Langmuir modeling of data, using C_{eq}*; duplicate series: #1 and #2).

available the reactive groups for La(III) sorption. At EDTA: 0.5 mM, Dy (III) is fully complexed and the further increase in EDTA concentration causes the progressive complexation of La(III), which becomes less sorbable. Therefore, at higher EDTA concentration the sorption capacity progressively decreases and becomes negligible when La(III) is fully complexed at EDTA: 1 mM.

These interpretations are confirmed by Fig. 6 where the sorption performances (and selectivity) are superposed to the speciation diagrams. Independently of the pH, the optimum EDTA concentration for selective recovery of La(III) corresponds to 0.5 mM where the La(III) begins to be complexed by EDTA (forming both LaEDTA⁻ and LaHEDTA⁻) while DyEDTA⁻ is fully formed. Therefore, the optimum EDTA concentration for separation of equimolar La(III) from Dy(III) is found at 0.5 mM EDTA concentration, for 1.0 mmol Ln L⁻¹ concentrations.

3.2.5. Extension to selective separation of La(III) from Er(III) and from Cu (II)

In order to verify these trends complementary investigations were performed with binary solutions containing either La(III)/Er(III) or La (III)/Cu(II). Erbium is another member of HREEs while Cu(II) is a representative of base metals frequently met in the leachates of WEEEs. Fig. 7a compares the sorption capacities and the selectivity coefficients in absence and presence of 0.5 mM EDTA at different pH₀ values (from 4

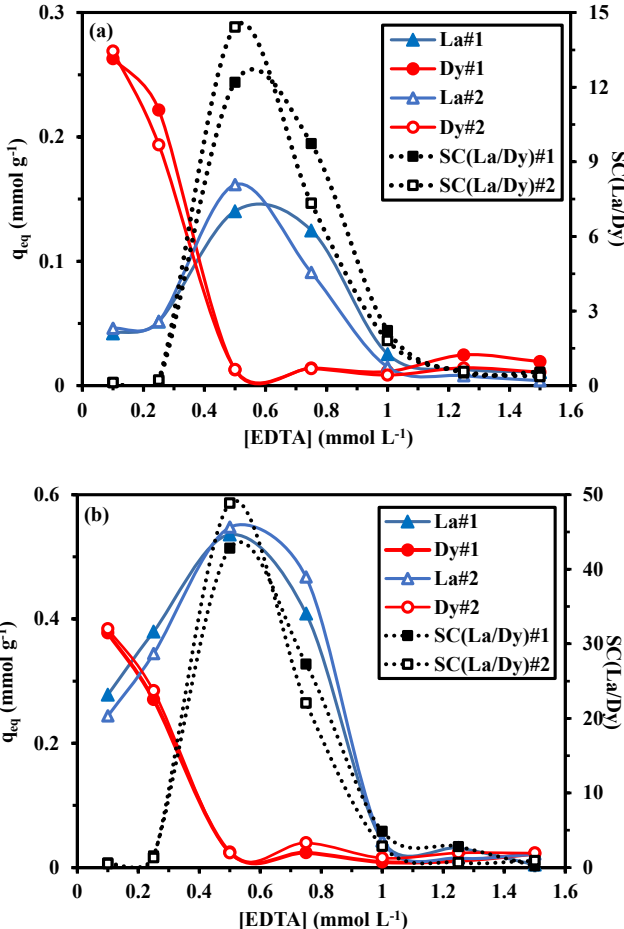


Fig. 5. Effect of EDTA concentration on La(III) and Dy(III) sorption capacities from binary equimolar solutions (C_0 : 0.5 mmol L⁻¹) and $SC_{La/Dy}$ at pH₀ 3 (a) and pH₀ 6 (b).

to 6). In absence of EDTA, both La(III) and Er(III) are efficiently bound:

(a) the equilibrium pH is significantly increased at pH₀ 4 and tends to level off at ~ 6.4 (the value reached at the other pH),

(b) the sorption capacities of Er(III) are roughly twice the levels reached for La(III), and

(c) the $SC_{La/Er}$ values range between 0.3 and 0.37 (meaning that AOEI has a preference for HREE against La(III), consistently with the results obtained with Dy(III)). However, this preference is relatively weak: $SC_{Er/La}$ does not exceed 3, making difficult their separation without making successive sorption/desorption steps [30].

The addition of EDTA completely changes the deal (Fig. 7b). As expected, in the continuity of La/Dy separation, the addition to EDTA improves the sorption of La(III) and almost inhibits Er(III) uptake. EDTA complexes Er(III), which, in turn, reduces the competition effect of HREE ions: sorption is almost doubled compared with EDTA-free solutions. The selectivity is completely reversed and strongly increased: $SC_{La/Er}$ increases with the pH from 25 to 39 when increasing pH₀ from 4 to 6 (pH_{eq}: 6.5–6.6). Fig. S23 shows the speciation diagrams for Ln(III) and EDTA in binary equimolar solutions. The stronger complexation of Er(III) by EDTA, compared with La(III), makes Er(III) poorly sorbable; enhancing the sorption and separation of La(III). These results confirm the scenario described for La(III)/Dy(III) separation.

The same procedure was applied to binary solutions containing La(III) and Cu(II) (Fig. 8). In absence of EDTA, the two metals are bound, with a significant preference of AOEI for copper: sorption capacities are poorly affected by the pH₀, ranging around 0.22–0.26 mmol La g⁻¹ and 0.43–0.54 mmol Cu g⁻¹. The $SC_{La/Cu}$ values (around 0.2) reflect the

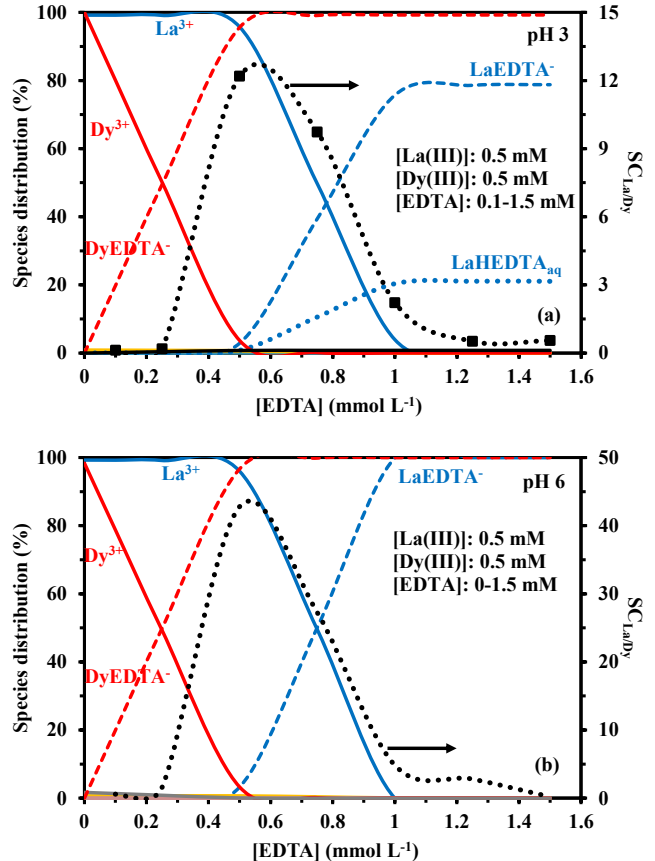


Fig. 6. Correlation between the $SC_{La/Dy}$ and La(III)-Dy(III) speciation diagrams at pH 3 (a) and pH 6 (b) for increasing concentrations of EDTA (C_0 : 0.5 mmol L⁻¹; example of correlation with Series #1 from Fig. 5).

preference of the sorbent for Cu(II) against La(III). According to the hard and soft acid base principle (HSAB, [68]), copper is part of the borderline class, contrary to Ln(III), which are considered hard acids. Hard acids preferentially react with hard bases (containing O and N ligands). The preference for Cu(II) is probably influenced by other parameters such as the ionic radius ($r(La)$: 1.216 Å $\gg r(Cu)$: 0.73 Å, [69]) and the cationic charge held by the metal ions (trivalent vs. divalent cations). The speciation of metal ions has a limited effect. Indeed, Fig. S24 shows the speciation diagrams for La(III) and Cu(II) in binary equimolar solutions (0.5 mmol L⁻¹), without EDTA. Free La³⁺ and Cu²⁺ largely predominate (>98.5%). With the addition of EDTA, contrary to Ln(III), the separation of La(III) from Cu(II) is not significantly improved. Indeed, the sorption capacity weakly increases (varying from 0.29 to 0.38 mmol La g⁻¹ with pH increases), while copper uptake is weakly reduced (in the range 0.33–0.42 mmol g⁻¹). The sorbent still maintains a preference for copper against lanthanum; $SC_{La/Cu}$ increases with the pH from 0.33 to 0.42. These values clearly show the difficulty to easily separate La(III) from Cu(II). Fig. S25 shows the speciation diagrams for La(III) and Cu(II) in binary solutions (equimolar 0.5 mmol L⁻¹) in the presence of EDTA (0.5 mM). The formation of copper complex does not allow the separation of the two metals (as it was observed for the separation of La(III) from HREEs). Lanthanum remains in the whole pH range in its free form (i.e., La³⁺), metal sorption is slightly increased with pH; and the sorption capacities are higher than for EDTA-free solutions. On the opposite hand, copper forms complexes with EDTA, which apparently are less sorbed: sorption capacity (compared with EDTA-free solutions) is decreased by 30–50%. The loss in sorption capacity is slightly higher at pH₀ 4, where co-exists CuHEDTA⁻ and CuEDTA²⁻. The complexation of Cu(II) slightly decreases the availability of sorbable copper species (free cationic forms); this causes both the weaker sorption of Cu(II) and the

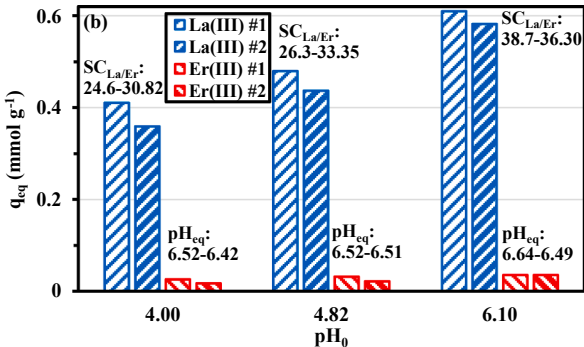
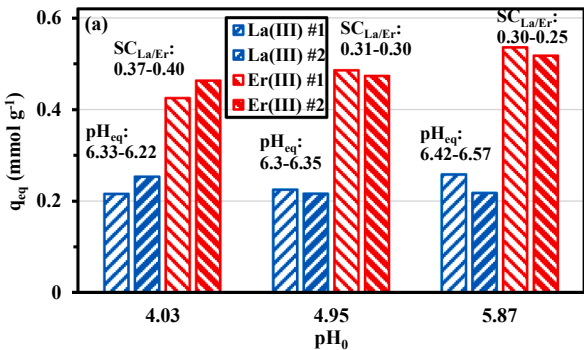


Fig. 7. Effect of pH_0 on La(III) and Er(III) sorption using AO-APEI beads from bi-component solutions in the absence (a) and in the presence (b) of EDTA (C_0 (metal): 0.5 mmol L⁻¹; EDTA concentration: 0.5 mmol L⁻¹ (when relevant); time: 48 h; SD: 0.5 g L⁻¹; additional information: equilibrium pH and $\text{SC}_{\text{La}/\text{Er}}$ values; duplicate series: #1 and #2).

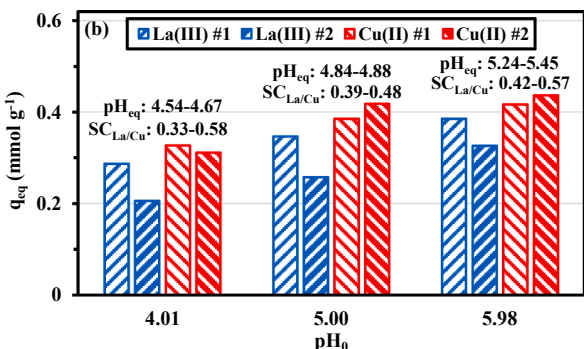
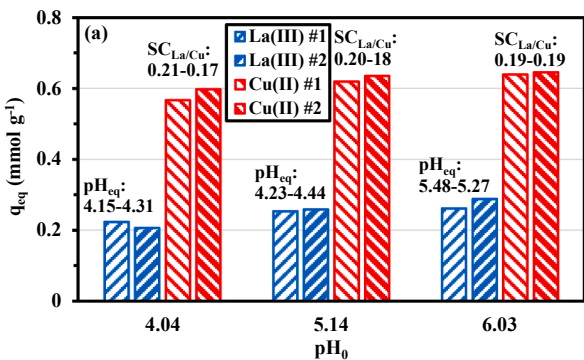


Fig. 8. Effect of pH_0 on La(III) and Cu(II) sorption using AO-APEI beads from bi-component solutions in the absence (a) and in the presence (b) of EDTA (C_0 (metal): 0.5 mmol L⁻¹; EDTA concentration: 0.5 mmol L⁻¹ (when relevant); time: 48 h; SD: 0.5 g L⁻¹; additional information: equilibrium pH and $\text{SC}_{\text{La}/\text{Cu}}$ values; duplicate series: #1 and #2).

slight increase in La(III) uptake (the competition of copper ions is less active). At pH 6, the predominant species are La^{3+} and CuEDTA^{2-} . In the case of Ln(III), the difference in EDTA complexation between La(III) and HREE(III) was sufficient for making possible the separation of LREE from HREE. This is not the case for the separation of La(III) from Cu(II). This cannot be explained by the EDTA stability constants that are very close for HREEs and for Cu(II) (i.e., $\log_{10} K(\text{MeEDTA})$: 18.78 for CuEDTA²⁻ chelates [70], 18.28 for DyEDTA⁻ chelates and 18.83 for ErEDTA⁻ chelates [60]). Cu-EDTA complexes maintain significant sorption levels onto AO-APEI (though lower than in absence of EDTA). The ionic radius of Cu(II) is much smaller than the values reported for the Ln (III) (see above) and the lower ionic charge may contribute to these differences in sorbability.

3.2.6. Metal desorption and sorbent recycling

Dysprosium desorption is highly efficient (>97%) while using 0.05 M CaCl_2 solution (at pH 2) (Fig. S26); while the desorption efficiency does not exceed 85% in the case of lanthanum. Acidic solution is favorable to the desorption of bound metal ions, while the presence of calcium contributes to stabilize the sorbent (ionotropic gelation of uronic groups of alginate-based material with calcium). The desorption equilibrium is achieved within 6 h of contact (Fig. S26). Alternatively, EDTA solutions (with increasing concentrations, from 0.1 to 1.5 mM) were used for desorbing the REEs. Dysprosium desorption by EDTA is globally more efficient than for lanthanum; indeed, lower EDTA concentration (i.e., 0.5 mM) is required for achieving the complete desorption of Dy(III) (compared with La(III); i.e., 1 mM) (Fig. S27). This is directly correlated to the greater affinity of EDTA for Dy(III) than for La(III) (stability constants). EDTA is displacing more easily dysprosium from the sorbent than lanthanum.

Fig. S28 compares the sorption capacities and desorption efficiencies for both La(III) and Dy(III) over 3 cycles using AO-APEI and different eluents (EDTA or CaCl_2 solutions). The sorption capacity systematically decreases with the recycling, partially due to the incomplete desorption that ranges between 80 and 93%. Globally, the decrease in desorption efficiency is less marked with CaCl_2 solutions, while at recycling the loss in sorption capacity is less marked than when using EDTA solution. These results are discussed in detail in Annex V (SI).

4. Conclusion

The amidoxidation of APEI beads enhances the sorptions of lanthanum and dysprosium, which are both preferentially sorbed at pH 5–6 (with maximum sorption capacities close to 0.56–0.6 mmol g⁻¹).

In binary solutions, despite the preference of the sorbent for dysprosium, the coefficient ($\text{SC}_{\text{La}/\text{Dy}}$) remains very low (i.e., 0.18–0.33), making difficult their separation. The addition of EDTA, which has a marked preference for complexing heavy REEs (such as Dy(III) and Er (III)), allows increasing the sorption of La(III): the selectivity coefficient increases up to 30–60. The optimal EDTA concentration for maximal selectivity corresponds to the stoichiometric concentration for full complexation of the HREE (for example: 0.5 mM for 0.5 mmol Dy L⁻¹ or 0.5 mmol Er L⁻¹). The sorbent preferentially sorbs free REE(III) species. The sorption isotherms are sigmoidal in the presence of EDTA, metal sorption begins when free metal species becomes to appear in the solution. Replacing total concentration with the effective concentration of adsorbable (free) metal species allows turning the sorption isotherm to the conventional highly favorable shape. The correlation of metal speciation in the presence of EDTA with sorption profiles confirms the predominance of this criterion over other conventional criteria such as metal radius, softness, electronegativity, and HSAB principles.

Playing with different soluble ligands (and macroligands), applying successive sorption/desorption cycles (with the eluate solutions) would be meaningful for enhancing the separation of the Ln(III) from complex multi-element solutions. These perspectives are under evaluation for designing novel separation processes.

Declaration of Competing Interest

The authors declare that they have no known competing financial interests or personal relationships that could have appeared to influence the work reported in this paper.

Acknowledgements

Y. Zhang acknowledges the China Scholarship Council (CSC, Grant N° 201906660008) for PhD fellowship.

Appendix A. Supplementary data

Supplementary data to this article can be found online at <https://doi.org/10.1016/j.cej.2021.133214>.

References

- [1] Y. Hu, J. Florek, D. Lariviere, F.-G. Fontaine, F. Kleitz, Recent advances in the separation of rare earth elements using mesoporous hybrid materials, *Chemical Record* 18 (2018) 1261–1276.
- [2] C. Erust, A. Akcil, A. Tuncuk, H. Deveci, E.Y. Yazici, A multi-stage process for recovery of neodymium (Nd) and dysprosium (Dy) from spent hard disc drives (HDDs), *Miner. Process. Extr. Metall. Rev.* 42 (2019) 99–101.
- [3] M. Sethurajan, E.D. van Hullebusch, D. Fontana, A. Akcil, H. Deveci, B. Batinic, J. P. Leal, T.A. Gasche, M.A. Kucuker, K. Kuchta, et al., Recent advances on hydrometallurgical recovery of critical and precious elements from end of life electronic wastes-a review, *Crit. Rev. Env. Sci. Technol.* 49 (2019) 212–275.
- [4] N. Swain, S. Mishra, A review on the recovery and separation of rare earths and transition metals from secondary resources, *J. Cleaner Prod.* 220 (2019) 884–898.
- [5] F. Xie, T.A. Zhang, D. Dreisinger, F. Doyle, A critical review on solvent extraction of rare earths from aqueous solutions, *Miner. Eng.* 56 (2014) 10–28.
- [6] S. Pavón, A. Fortuny, M.T. Coll, A.M. Sastre, Rare earths separation from fluorescent lamp wastes using ionic liquids as extractant agents, *Waste Manage. (Oxford)* 82 (2018) 241–248.
- [7] S. Pavón, A. Fortuny, M.T. Coll, A.M. Sastre, Solvent extraction modeling of Ce/Eu/Y from chloride media using D2EHPA, *AIChE J.* 65 (8) (2019) e16627.
- [8] J. Wang, Adsorption of aqueous neodymium, europium, gadolinium, terbium, and yttrium ions onto nZVI-montmorillonite: kinetics, thermodynamic mechanism, and the influence of coexisting ions, *Environ. Sci. Pollut. Res.* 25 (2018) 33521–33537.
- [9] T. Kegl, A. Kosák, A. Lobník, Z. Novák, A.K. Kralj, I. Ban, Adsorption of rare earth metals from wastewater by nanomaterials: a review, *J. Hazard. Mater.* 386 (2020) 121632.
- [10] D. Fila, Z. Hubicki, D. Kolodynska, Recovery of metals from waste nickel-metal hydride batteries using multifunctional diphenox resin, *Adsorption (J. Int. Ads. Soc.)* 25 (2019) 367–382.
- [11] D. Kolodynska, D. Fila, Z. Hubicki, Static and dynamic studies of lanthanum(III) ion adsorption/desorption from acidic solutions using chelating ion exchangers with different functionalities, *Environ. Res.* 191 (2020), 110171.
- [12] D. Kolodynska, D. Fila, Z. Hubicki, Evaluation of possible use of the macroporous ion exchanger in the adsorption process of rare earth elements and heavy metal ions from spent batteries solutions, *Chem. Eng. Process. Process Intensif.* 147 (2020), 107767.
- [13] D. Gomes Rodrigues, S. Monge, S.p. Pellet-Rostaing, N. Dacheux, D. Bouyer, C. Faur, Sorption properties of carbamoylmethylphosphonated-based polymer combining both sorption and thermosensitive properties: New valuable hydrosoluble materials for rare earth elements sorption, *Chem. Eng. J.*, 355 (2019) 871–880.
- [14] D.D. Miller, R. Siriwardane, D. McIntyre, Anion structural effects on interaction of rare earth element ions with Dowex 50W X8 cation exchange resin, *J. Rare Earths* 36 (2018) 879–890.
- [15] X. Heres, V. Blet, P. Di Natale, A. Ouaattou, H. Mazouz, D. Dhiba, F. Cuer, Selective extraction of rare earth elements from phosphoric acid by ion exchange resins, *Metals* 8 (2018) 8090682.
- [16] K. Araucz, A. Aurich, D. Kolodynska, Novel multifunctional ion exchangers for metal ions removal in the presence of citric acid, *Chemosphere* 251 (2020), 126331.
- [17] A.B. Botelho Junior, E.F. Pinheiro, D.C.R. Espinosa, J.A.S. Tenorio, M.d.P.G. Baltazar, Adsorption of lanthanum and cerium on chelating ion exchange resins: kinetic and thermodynamic studies, *Sep. Sci. Technol.*, (2021) doi: 10.1080/01496395.01492021.01884720.
- [18] E.O. Opare, E. Struhs, A. Mirkouei, A comparative state-of-technology review and future directions for rare earth element separation, *Renewable Sustainable Energy Rev.* 143 (2021), 110917.
- [19] A.B. Botelho Junior, D.C.R. Espinosa, J. Vaughan, J.A.S. Tenório, Recovery of scandium from various sources: A critical review of the state of the art and future prospects, *Miner. Eng.*, 172 (2021) 107148.
- [20] M. Hermassi, M. Granados, C. Valderrama, C. Ayora, J.L. Cortina, Recovery of rare earth elements from acidic mine waters by integration of a selective chelating ion-exchanger and a solvent impregnated resin, *J. Environ. Chem. Eng.* 9 (2021), 105906.
- [21] J. Lie, J.-C. Liu, Selective recovery of rare earth elements (REEs) from spent NiMH batteries by two-stage acid leaching, *J. Environ. Chem. Eng.* 9 (2021), 106084.
- [22] M. Karve, B. Vaidya, Selective separation of scandium(III) and yttrium(III) from other rare earth elements using cyanex302 as an extractant, *Sep. Sci. Technol.* 43 (2008) 1111–1123.
- [23] S.M. Xaba, M. Nete, W. Purcell, Concentration of rare earth elements from monazite by selective precipitation, in: S. Chikosha, R. Machaka (Eds.), Conference of the South African Advanced Materials Initiative, 2018, p. pp., <https://doi.org/10.1088/1757-1899x/1430/1081/012006>.
- [24] D. Prodius, M. Klocke, V. Smetana, T. Alammar, M.P. Garcia, T.L. Windus, I. C. Nlebedim, A.-V. Mudring, Rationally designed rare earth separation by selective oxalate solubilization, *Chem. Commun.* 56 (2020) 11386–11389.
- [25] Z.C. Wang, Y.H. Sun, A stepwise selective chlorination-chemical vapor transport reaction for rare earth separation, *Chem. Lett.* 26 (11) (1997) 1113–1114.
- [26] T. Uda, K.T. Jacob, M. Hirasawa, Technique for enhanced rare earth separation, *Science* 289 (2000) 2326–2329.
- [27] K.M. Lyons, J.P. Downey, J.L. Chorney, K.J. Schumacher, Selective Separation of Rare Earth Chlorides Utilizing Vapor Phase Extraction, 2017, 55–63 pp.
- [28] L.B. Jose, A.C.Q. Ladeira, Recovery and separation of rare earth elements from an acid mine drainage-like solution using a strong acid resin, *J. Water Process Eng.* 41 (2021), 102052.
- [29] J. Florek, F. Chalifour, F. Bilodeau, D. Larivière, F. Kleitz, Nanostructured hybrid materials for the selective recovery and enrichment of rare earth elements, *Adv. Funct. Mater.* 24 (2014) 2668–2676.
- [30] S.D.N. Almeida, H.E. Toma, Neodymium(III) and lanthanum(III) separation by magnetic nanohydrometallurgy using DTPA functionalized magnetite nanoparticles, *Hydrometallurgy*, 161 (2016) 22–28.
- [31] J. Florek, A. Mushaq, D. Larivière, G. Cantin, F.-G. Fontaine, F. Kleitz, Selective recovery of rare earth elements using chelating ligands grafted on mesoporous surfaces, *RSC Adv.* 5 (126) (2015) 103782–103789.
- [32] J. Roosen, J. Spooren, K. Binnemans, Adsorption performance of functionalized chitosan-silica hybrid materials toward rare earths, *J. Mater. Chem. A* 2 (45) (2014) 19415–19426.
- [33] J. Roosen, K. Binnemans, Adsorption and chromatographic separation of rare earths with EDTA- and DTPA-functionalized chitosan biopolymers, *J. Mater. Chem. A* 2 (5) (2014) 1530–1540.
- [34] F. Zhao, E. Repo, Y. Meng, X. Wang, D. Yin, M. Sillanpaa, An EDTA-beta-cyclodextrin material for the adsorption of rare earth elements and its application in preconcentration of rare earth elements in seawater, *J. Colloid Interface Sci.* 465 (2016) 215–224.
- [35] T. Suzuki, K. Itoh, A. Ikeda, M. Aida, M. Ozawa, Y. Fujii, Separation of rare earth elements by tertiary pyridine type resin, *J. Alloys Compd.* 408–412 (2006) 1013–1016.
- [36] Y. Tomobuchi, Y. Tachibana, M. Nomura, T. Suzuki, Effect of alcohols on separation behavior of rare earth elements using benzimidazole-type anion-exchange resin in nitric acid solutions, *J. Radioanal. Nucl. Chem.* 303 (2015) 1425–1428.
- [37] T. Hirai, I. Komasa, Extraction and separation of rare-earth elements by tri-n-octylmethylammonium nitrate and β-diketone using water-soluble complexing agent, *J. Chem. Eng. Jpn.* 24 (1991) 731–736.
- [38] J. Kovalancik, M. Galova, Extraction separation of rare-earth elements by amines in the presence of complexing agents, *J. Radioanal. Nucl. Chem.* 162 (1992) 35–46.
- [39] J. Kovalancik, M. Galova, Extraction separation of rare-earth elements by amines in the presence of complexing agents Pt 2, *J. Radioanal. Nucl. Chem.* 162 (1992) 47–56.
- [40] S. Chen, M. Xiao, D. Lu, X. Zhan, Carbon nanofibers as solid-phase extraction adsorbent for the preconcentration of trace rare earth elements and their determination by inductively coupled plasma mass spectrometry, *Anal. Lett.* 40 (2007) 2105–2115.
- [41] R.D. Gomes, L.A. Seruff, M.L. Wainerach Scal, Y.M. Vera, The Influence of lactic acid concentration on the separation of light rare earth elements by continuous liquid-liquid extraction with 2-ethylhexyl phosphonic acid mono-2-ethylhexyl ester, *Metall. Mater. Trans. B* 49 (2018) 460–465.
- [42] E. Kashi, R. Habibpour, H. Gorzin, A. Maleki, Solvent extraction and separation of light rare earth elements (La, Pr and Nd) in the presence of lactic acid as a complexing agent by Cyanex 272 in kerosene and the effect of citric acid, acetic acid and Titriplex III as auxiliary agents, *J. Rare Earths* 36 (2018) 317–323.
- [43] A. Kumari, K.K. Sahu, S.K. Sahu, Solvent extraction and separation of Nd, Pr and Dy from leach liquor of waste NdFeB magnet using the nitrate form of Mextral® 336At in the presence of aquo-complexing agent EDTA, *Metals* 9 (2019) 269.
- [44] F. Zhang, X. Sun, J. Wang, Q. Zhang, S. Sun, Extraction enhancement and mechanism of light rare-earth elements (III) in chloride medium through adding complexing agent and synergistic effect, *Sep. Sci. Technol.* 55 (2020) 3375–3385.
- [45] E.J. Wheelwright, F.H. Spedding, The use of chelating agents in the separation of the rare earth elements by ion-exchange methods, in, Ames Laboratory ISC Technical Reports. 101., Ames (IA), USA, 1955, pp. 92 pp.
- [46] R.S. Dybczynski, K. Kulisa, Separation of rare earth elements (REE) by ion interaction chromatography (IIC) using diglycolic acid (ODA) as a complexing agent, *Chromatographia* 84 (2021) 473–482.
- [47] A. Zhang, E. Kuraoka, M. Kumagai, Preparation of a novel macroporous silica-based 2,6-bis(5,6-diisobutyl-1,2,4-triazine-3-yl)pyridine impregnated polymeric composite and its application in the adsorption for trivalent rare earths, *J. Radioanal. Nucl. Chem.* 274 (2007) 455–464.
- [48] H. Hubicka, D. Drobek, Anion-exchange method for separation of ytterbium from holmium and erbium, *Hydrometallurgy* 47 (1997) 127–136.

- [49] H. Hubicka, Investigation of polyacrylate anion-exchangers for separation of rare earth element complexes with EDTA, *J. Rare Earths* 20 (2002) 31–35.
- [50] G. Zhou, Q. Li, P. Sun, W. Guan, G. Zhang, Z. Cao, L. Zeng, Removal of impurities from scandium chloride solution using 732-type resin, *J. Rare Earths* 36 (2018) 311–316.
- [51] J. Guzman, I. Saucedo, J. Revilla, R. Navarro, E. Guibal, Copper sorption by chitosan in the presence of citrate ions: influence of metal speciation on sorption mechanism and uptake capacities, *Int. J. Biol. Macromol.* 33 (2003) 57–65.
- [52] S. Wang, T. Vincent, C. Faur, E. Rodriguez-Castellon, E. Guibal, A new method for incorporating polyethyleneimine (PEI) in algal beads: high stability as sorbent for palladium recovery and supported catalyst for nitrophenol hydrogenation, *Mater. Chem. Phys.* 221 (2019) 144–155.
- [53] M.F. Hamza, K.A.M. Salih, A.A.H. Abdel-Rahman, Y.E. Zayed, Y. Wei, J. Liang, E. Guibal, Sulfonic-functionalized algal/PEI beads for scandium, cerium and holmium sorption from aqueous solutions (synthetic and industrial samples), *Chem. Eng. J.* 403 (2021), 126399.
- [54] M.F. Hamza, Y. Wei, E. Guibal, Quaternization of algal/PEI beads (a new sorbent): characterization and application to scandium recovery from aqueous solutions, *Chem. Eng. J.* 383 (2020), 123210.
- [55] Y. Wei, K.A.M. Salih, K. Rabie, K.Z. Elwakeel, Y.E. Zayed, M.F. Hamza, E. Guibal, Development of phosphoryl-functionalized algal-PEI beads for the sorption of Nd (III) and Mo(VI) from aqueous solutions – application for rare earth recovery from acid leachates, *Chem. Eng. J.* 412 (2021), 127399.
- [56] Y. Wei, K.A.M. Salih, M.F. Hamza, T. Fujita, E. Rodríguez-Castellón, E. Guibal, Synthesis of a new phosphonate-based sorbent and characterization of its interactions with lanthanum (III) and terbium (III), *Polymers* 13 (2021) 1513.
- [57] Y. Wei, K.A.M. Salih, S. Lu, M.F. Hamza, T. Fujita, T. Vincent, E. Guibal, Amidoxime functionalization of algal/polyethyleneimine beads for the sorption of Sr(II) from aqueous solutions, *Molecules* 24 (2019) 3893.
- [58] A.H. Zyoud, A. Zubi, S.H. Zyoud, M.H. Hilal, S. Zyoud, N. Qamhieh, A. Hajamohideen, H.S. Hilal, Kaolin-supported ZnO nanoparticle catalysts in self-sensitized tetracycline photodegradation: zero-point charge and pH effects, *Appl. Clay Sci.* 182 (2019), 105294.
- [59] P.M. Marcos, J.R. Ascenso, M.A.P. Segurado, R.J. Bernardino, P.J. Cragg, Synthesis, binding properties and theoretical studies of p-tert-butylhexahomotrioxacalix 3 arene tri(adamantyl)ketone with alkali, alkaline earth, transition, heavy metal and lanthanide cations, *Tetrahedron* 65 (2009) 496–503.
- [60] A. Hu, S.N. MacMillan, J.J. Wilson, Macroyclic ligands with an unprecedented size-selectivity pattern for the lanthanide ions, *JACS* 142 (2020) 13500–13506.
- [61] M. Torab-Mostaedi, M. Asadollahzadeh, A. Hemmati, A. Khosravi, Biosorption of lanthanum and cerium from aqueous solutions by grapefruit peel: equilibrium, kinetic and thermodynamic studies, *Res. Chem. Intermed.* 41 (2013) 559–573.
- [62] M. Torab-Mostaedi, Biosorption of lanthanum and cerium from aqueous solutions using tangerine (*Citrus reticulata*) peel: equilibrium, kinetic and thermodynamic studies, *Chem. Ind. Chem. Eng. Q.* 19 (2013) 79–88.
- [63] K. Vijayaraghavan, M. Sathishkumar, R. Balasubramanian, Biosorption of lanthanum, cerium, europium, and ytterbium by a brown marine alga, *Turbinaria conoides*, *Ind. Eng. Chem. Res.* 49 (2010) 4405–4411.
- [64] J.E. Gargari, H.S. Kalal, A. Shakeri, A. Khanchi, Synthesis and characterization of Silica/polyvinyl imidazole/H₂PO₄-core-shell nanoparticles as recyclable adsorbent for efficient scavenging of Sm(III) and Dy(III) from water, *J. Colloid Interface Sci.* 505 (2017) 745–755.
- [65] R. Qadeer, J. Hanif, Adsorption of dysprosium ions on activated-charcoal from aqueous solutions, *Carbon* 33 (1995) 215–220.
- [66] E. Guibal, C. Milot, J. Roussy, Influence of hydrolysis mechanisms on molybdate sorption isotherms using chitosan, *Sep. Sci. Technol.* 35 (2000) 1021–1038.
- [67] J. Guzman, I. Saucedo, R. Navarro, J. Revilla, E. Guibal, Vanadium interactions with chitosan: influence of polymer protonation and metal speciation, *Langmuir* 18 (2002) 1567–1573.
- [68] R.G. Pearson, Acids and bases 151 (1966) 172–177.
- [69] I. Persson, Hydrated metal ions in aqueous solution: How regular are their structures? *Pure Appl. Chem.* 82 (2010) 1901–1917.
- [70] M.J.A. Lima, B.F. Reis, E.A.G. Zagatto, M.Y. Kamogawa, An automatic titration setup for the chemiluminometric determination of the copper complexation capacity in opaque solutions, *Talanta* 209 (2020), 120530.
- [71] D. Dupont, W. Brullot, M. Bloemen, T. Verbiest, K. Binnemans, Selective uptake of rare earths from aqueous solutions by EDTA-functionalized magnetic and nonmagnetic nanoparticles, *ACS Appl. Mater. Interfaces* 6 (7) (2014) 4980–4988.
- [72] E. Polido Legaria, M. Samouhos, V.G. Kessler, G.A. Seisenbaeva, Toward molecular recognition of REEs: comparative analysis of hybrid nanoadsorbents with the different complexation ligands EDTA, DTPA, and TTHA, *Inorg. Chem.* 56 (22) (2017) 13938–13948.
- [73] D. Dupont, J. Luyten, M. Bloemen, T. Verbiest, K. Binnemans, Acid-stable magnetic core-shell nanoparticles for the separation of rare earths, *Ind. Eng. Chem. Res.* 53 (39) (2014) 15222–15229.
- [74] D. Wu, Y. Sun, Q. Wang, Adsorption of lanthanum (III) from aqueous solution using 2-ethylhexyl phosphonic acid mono-2-ethylhexyl ester-grafted magnetic silica nanocomposites, *J. Hazard. Mater.* 260 (2013) 409–419.
- [75] S. Yang, P. Zong, X. Ren, Q. Wang, X. Wang, Rapid and highly efficient preconcentration of Eu(III) by core-shell structured Fe₃O₄@humic acid magnetic nanoparticles, *ACS Appl. Mater. Interfaces* 4 (12) (2012) 6891–6900.
- [76] A.E. Oral, S. Aytas, S. Yusun, S. Sert, C. Gok, O. Elmastaş Gultekin, Preparation and characterization of a graphene-based magnetic nanocomposite for the adsorption of lanthanum ions from aqueous solution, *Anal. Lett.* 53 (11) (2020) 1812–1833.
- [77] Q. Zhao, Y. Wang, Z. Xu, Z. Yu, The potential use of straw-derived biochar as the adsorbent for La(III) and Nd(III) removal in aqueous solutions, *Environ. Sci. Pollut. Res.* 28 (34) (2021) 47024–47034, <https://doi.org/10.1007/s11356-021-13988-2>.
- [78] L. Alcaraz, María E. Escudero, F. José. Alguacil, I. Llorente, A. Urbíeta, P. Fernández, Félix A. López, Dysprosium removal from water using active carbons obtained from spent coffee ground, *Nanomaterials* 9 (10) (2019) 1372, <https://doi.org/10.3390/nano101372>.
- [79] K. Kondo, M. Umetsu, M. Matsumoto, Adsorption characteristics of gadolinium and dysprosium with microcapsules containing an extractant, *J. Water Process Eng.* 7 (2015) 237–243.